PROCEEDINGS OF SPIE

SPIEDigitalLibrary.org/conference-proceedings-of-spie

Exploration of uncooled quantum infrared detectors based on quantum dots/graphene heterostructures

Wu, Judy

Judy Z. Wu, "Exploration of uncooled quantum infrared detectors based on quantum dots/graphene heterostructures," Proc. SPIE 11407, Infrared Technology and Applications XLVI, 1140706 (23 April 2020); doi: 10.1117/12.2556930

SPIE.

Event: SPIE Defense + Commercial Sensing, 2020, Online Only

Exploration of uncooled quantum infrared detectors based on quantum dots/graphene heterostructures

Judy Z. Wu*[a]
[a]Department of Physics and Astronomy, University of Kansas, Lawrence, KS USA 66045

ABSTRACT

Heterojunction nanohybrids based on low-dimension semiconductors, including colloidal quantum dots (QDs) and 2D atomic materials (graphene, transition metal chalcogenides, etc) provide a fascinating platform to design of new photonic and optoelectronic devices that take advantages of the enhanced light-solid interaction attributed to their strong quantum confinement and superior charge mobility for uncooled photodetectors with a high gain up to 10^{10}. In these heterojunction nanohybrids, the van der Waals (vdW) interface plays a critical role in controlling the optoelectronic process including exciton dissociation by the interface built-in field that drives the follow-up charge injection and transport to graphene. In this paper, we present our recent progress in development of such heterostructures nanohybrids for uncooled infrared detectors including PbS and FeS_2 QDs/graphene and 2D vdW heterostructures $MoTe_2$/Graphene/SnS_2 and GaTe/InSe. We have found that nonstoichiometric $Fe_{1-x}S_2$ QDs (x = 0.01–0.107) with strong localized surface plasmonic resonance (LSPR) can have much enhanced absorption in broadband from ultraviolet to short-wave infrared (SWIR, 1–3 μm). Consequently, the LSPR $Fe_{1-x}S_2$ QDs/graphene heterostructure photodetectors exhibit extraordinary photoresponsivity in exceeding 4.32×10^6 A/W and figure-of-merit detectivity D* > 7.50×10^{12} Jones in the broadband of UV–Vis–SWIR at room temperature. The 2D vdW heterostructures allows novel designs of interface band alignments with uncooled NIR-SWIR D* up to 10^{12} Jones. These results illustrate that the heterostructure nanohybrids provide a promising pathway for low-cost, printable and flexible infrared detectors and imaging systems.

Keywords: Quantum dots, graphene, 2D atomic materials, heterojunction, nanohybrids, plasmonic, infrared detectors

1. INTRODUCTION

Optoelectronic nanohybrids involving graphene and quantum nanostructures have recently emerged as a unique scheme for high-performance photodetection.[1] Graphene has attracted extensive attention due to its unique electronic structure,[2-5] two dimensional (2D) nature, ultrahigh mobility (up to 4×10^4 $cm^{-2}V^{-1}s^{-1}$ for unsuspended graphene at room temperature)[6, 7], flexibility and chemical stability. The nanostructures are photosensitizers with morphologies of quantum dots (0D),[8-13] nanotubes and nanowires (1D)[14, 15] and nanosheets (2D) such as transition metal dichalcogenides (TMDC).[16-18] The implementation of graphene or other 2D atomic sheets of extraordinary charge carrier mobility in the nanohybrids makes a fundamental difference in the carrier transport in the nanohybrids optoelectronics as compared to the counterparts based on the nanostructures only. In the quantum dots (QDs) photodetectors, for example, the quantum confinement in QDs due to the suppressed phonon scattering[19] is expected to reduce dark current and hence improve the detector performance,[20, 21] which has been shown experimentally on colloidal HgTe QDs with surface passivation[22-24] and InSb-nanowires.[25, 26] However, the low carrier mobility in the range of 10^{-6} $cm^{-2}V^{-1}s^{-1}$ (in as-made HgTe QDs) to 10^{-4} $cm^{-2}V^{-1}s^{-1}$ (with ligand exchange on HgTe QDs to passivate the surface defects) IR detectors remains a bottleneck towards obtaining high detectivity D* in QD-based IR detectors.[24] This bottleneck can be removed by combining the narrow-bandgap QDs with graphene field-effect transistors (GFETs), taking advantages of the high mobility > $4x10^4$ $cm^{-2}V^{-1}s^{-1}$ in graphene at room temperature. As we have shown recently, D* improvement by orders of magnitude can be achieved in QD/GFET as compared to QD only photodetectors.[9, 27] Microscopically, excitons generated through light absorption by the QDs will be dissociated by the build-in field into free carriers at the QD/graphene interface, followed with carrier transfer from QDs to graphene for high-mobility carrier transport to electrodes. This can significantly reduce the charge recombination stemming from the low mobility of the QDs and QD-QD junctions. Therefore, the nanostructure/graphene heterostructures nanohybrids approach may provide a unique scheme for high-sensitivity photodetectors by taking advantage of the quantum confinement of the semiconductor nanostructures with ballistic charge transport in graphene to enable unprecedented performance.

Infrared Technology and Applications XLVI, edited by Bjørn F. Andresen, Gabor F. Fulop, John Lester Miller, Lucy Zheng, Proc. of SPIE Vol. 11407, 1140706 · © 2020 SPIE
CCC code: 0277-786X/20/$21 · doi: 10.1117/12.2556930

Fig. 1 illustrates three examples of the nanohybrid photodetectors demonstrated using QDs,[8-13] nanowires,[28] and nanosheets[29, 30] as photosensitizers. Upon light absorption by the sensitizer, excitons (electron-hole pairs) are generated and separated by the build-in field at the nanostructure/graphene interface. Driven by the build-in field, one type of photo-excited carriers in the QDs (or other nanostructures with equivalent quantum confinement) are transferred into graphene across the nanohybrid interface and circulate many times between electrodes within the lifetime of the excitons in the QDs due to the high mobility of graphene, resulting in high external quantum efficiency (EQE) due to a high photoconductive gain up to 10^{10} defined as gain=τ_c/τ_t,[8, 9, 29] where τ_c is the exciton life time in the QD (or other nanostructures) and τ_t is the carrier transit time in the photoconductive GFET channel between electrodes. The transit time $\tau_t = l^2/\mu_c V_{bias}$ is proportional to the square of the GFET channel length l and inversely proportional to the carrier mobility μ_c in graphene and the bias voltage (source-drain in GFET) V_{bias}. Thus the high gain in the QD/GFET devices is the combination of the advantages of strong quantum confinement in QDs (high τ_c) and the high mobility μ_c (up to 4×10^4 $cm^{-2}V^{-1}s^{-1}$ for unsuspended graphene at room temperature)[6, 7] in graphene (low τ_t). In contrast to QD-based photodetectors (without graphene) that are limited by the low carrier mobility in the range of 10^{-6} $cm^{-2}V^{-1}s^{-1}$ to 10^{-4} $cm^{-2}V^{-1}s^{-1}$,[24] the high mobility in graphene by 8-10 orders of magnitude is claimed a key factor facilitating the high gain up to 10^{10} reported in various nanostructure/GFET nanohybrid photodetectors and represents an unique advantage of the nanohybrid photodetectors.[8, 9, 29]

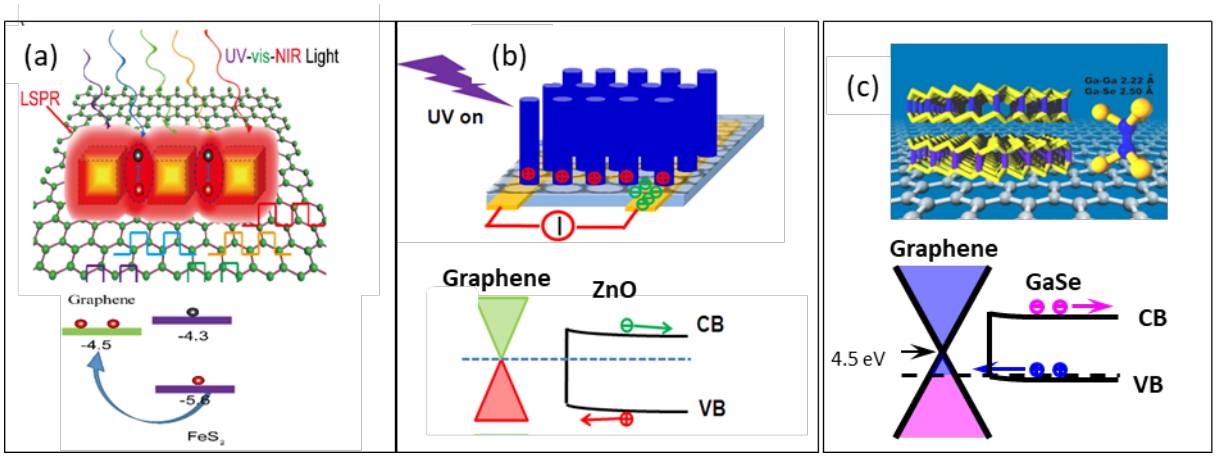

Figure 1. Schematic of three types of sensitizer/graphene nanohybrids photodetectors with build-in fields designed at the sensitizer/graphene interface to facilitate exciton separation and charge transfer in: (a) plasmonic 0D FeS_2 quantum dots/graphene; (b) 1D ZnO nanowire/graphene; and (c) 2D GeSe nanosheet/graphene for high gain in the range of 10^6 to 10^{10}.

Another advantage of the nanohybrids photodetectors is attributed to the strong quantum confinement in the nanostructured photosensitizers, which not only contributes to the high gain as discussed above, but also allows bandgap (E_g) and hence spectral tunability through control of the shape, dimension, stacking (2D stacks and core/shell QDs), and carrier doping for localized surface plasmonic resonance (LSPR).[31] The LSPR FeS_2 QDs shown in **Fig. 1a** presents an excellent example with not only much enhanced photoresponse but also much expanded spectral range from UV to short-wave infrared (SWIR) via doping or/and shape control for broadband photodetection using FeS_2 QD/GFET nanohybrids.[32]

Moreover, the GFET gate provides another advantage in shifting the Fermi energy of graphene with respect to the conduction and valence bands of the sensitizers (see insets at bottom of **Fig. 1** for each of the three devices) for an optimal interface build-in field for exciton dissociation and charge transfer across the sensitizer/GFET interface.[8, 9]

Finally, highly crystalline colloidal QDs and many other nanostructured sensitizers can be synthesized with controllable dimension, morphology and chemical composition using low-cost, non- (or low)-vacuum processes. This provides an additional advantage towards commercial applications and allows integration of with Si-based readout circuits using inkjet printing the nanostructure sensitizers.[14, 33-35]

These advantages make sensitizer/graphene nanohybrids highly promising for designing uncooled quantum infrared (IR) detectors that have been widely used in both commercial and military applications.[36-40] with high detectivity, high speed, low-cost and scalability. Motivated by this, we have explored several nanohybrids for IR detection based on QDs and 2D atomic materials stacks. D* close to $1.0x10^{13}$ cm·Hz$^{1/2}$/W in short-wave infrared (SWIR) spectrum, together with photoconductive gain up to 10^{10} illustrate that the combination of the advantages of strong quantum confinement in nanostructured absorber and the extraordinary carrier mobility in graphene provides fresh opportunities in exploration of the uncooled IR detection. In the following, we will discuss our experimental results.

2. EXPERIMENTAL

2.1 Synthesis of graphene and other 2D atomic materials

CVD was deployed for synthesis of graphene in large area either on commercial copper foils[41, 42] or on SiO_2/Si substrates.[43] In the former, the copper foil must be removed using a graphene transfer protocol[44] to transfer graphene on various substrates for device applications. The advantage of the transfer is almost any substrates could be considered for devices, which is particularly important to those, such as polymers or plastics, with a low thermal budgets incompatible to the CVD growth temperatures typically in exceeding 1000 °C. However, graphene transfer process is prone for surface contamination by various chemical and solvent residues which can affect the interface of the heterojunction nanohybrid optoelectronics through formation of charge traps at the interface, which can degrade the optoelectronic performance by blocking the charge transfer (low responsivity and detectivity D*) as well as slow down the photoresponse (asymmetric and long response times). Transfer-free, direct CVD growth of graphene can effectively resolve the issues associated caused in graphene transfer, resulting indeed improved optoelectronic performance as to be discussed in this paper. However, high quality CVD graphene has only been reported on a limited number of substrates, such as SiO_2/Si, quartz and fused silica in a narrower temperature window as compared to that for CVD graphene on copper foils, which is attributed to the more difficult nucleation of graphene without metal catalyst (such as copper).

CVD growth of 2D atomic materials on graphene, such as TMDCs, allow layer-by-layer deposition in large area, which is important to the practical applications.[30] An additional benefit is a clean interface formed between TMDC and graphene, especially the transfer-free graphene. In the TMDC growth, both continuous atomic sheets of monolayer and few layers[30, 45] and nano-discs of tens to hundreds of nm in diameter[46-48] have been obtained successfully. It is particularly worth mentioned that the latter are confirmed to exhibit localized surface plasmonic resonance (LSPR) and hence significantly enhanced light absorption/trapping due to a so-called photo-doping facilitated by the TMDC/graphene interface as suggested by a Density Function Theory (DFT) simulation.[46-48] The benefit of these non-metal plasmonic nanostructures is in their inherent low loss. In fact, this argument is supported by the higher sensitivity of the TMDC-NDs/graphene, as compared with Au-NPs/graphene, in surface enhanced Raman spectroscopy of biomolecules, and higher responsivity in TMDC-NDs/graphene photodetectors in comparison with the TMDC-CL/graphene counterpart's.

For exploration of heterostructures of monolayer or/and few-layers of different 2D atomic materials whose growth remains challenging so far, mechanical exfoliation of flakes from their bulk crystals was deployed, followed with stacking them in designed sequences for the anticipated interface band edge alignments. Considering the small dimension of the flakes typically in the range few to tens of μm, advanced lithography is required to lay electrodes for optoelectronic devices.

2.2 Synthesis and surface engineering of colloidal quantum dots

Colloidal fabrication of QDs of various semiconductors have been intensively studied. For IR detection, semiconductors with low band gaps suitable for different IR bands are typically selected. It should be realized that QDs with their dimension on the other of few to few tens of nm, have a large surface to volume ratio. The large surface area on low-band gap semiconductor QDs implies surface defects that may cause degradation in ambient and poor interfaces both at the QD-QD junctions and on the QD/graphene nanohybrid interface. Ligand exchange provides a common solution to this problem by passivating the dangling chemical bonds on the QD surfaces. In the QD/graphene nanohybrid optoelectronic devices, an additional role is required in ligand exchange for the ligand molecules to form efficient charge transport channels at QD-QD and QD/graphene interfaces for high and fast photoresponse. For example, 3-

mercaptopropionic acid (MPA) ligands have been found experimentally, as well as DFT simulation, to provide both passivation of the QDs and form the efficient charge transfer channels.[10, 49]

Another challenge in QD/graphene nanohybrids is associated to the limited light absorption by a thin layer (a monolayer or a few layer of QDs) of QDs in the nanohybrids. It should be noted increasing the QD thickness is not a good solution due to the limited QD-QD charge transport.[12] One scheme to address this issue is through coupling of plasmon nanostructures to the QD/graphene nanohybrids. For example, a plasmonic AgNPs-metafilm coupled with a thin (10-20 nm) insulting spacer to the nanohybrids has been found to enhance the photoresponse of the nanohybrid photodetectors by >7 times.[50] Keep in mind this would require additional fabrication steps. Another scheme is to make plasmonic QDs via carrier doping,[31] which has been found to not only provide remarkably enhanced light absorption by the QDs, but also the red shift of the cutoff much beyond the limit by the band gap into the IR spectrum. In comparison with the QDs of lower band gap semiconductors for IR detection, the plasmonic QDs of larger band gaps, such as iron pyrites[51, 52] (Eg in visible) and lead sulfites (Eg in NIR), have a unique advantage of much enhanced light absorption in broadband extended to IR spectrum, which allows much improved responsivity and D* to be obtained in NIR-SWIR spectral range.

2.3 Fabrication of vdW heterostructures nanohybrids

In this work, several different processes have been developed for fabrication of the vdW heterostructures nanohybrids. These processes can be divided into two types: direct growth using CVD or solution method, and mechanical stacking using drop-casting, spin-coating and inkjet printing. In both approaches, a control of the vdW interface is the key in achievement of the heterostructure nanohybrids for high-performance photodetectors and other optoelectronics since the interface provides the built-in field for exciton dissociation into free charge carriers and the follow-up charge transfer. Considering such a control must be at an atomic resolution, several post interface-cleaning processes have been explored and among them light-assisted vacuum annealing,[29, 53] ligand exchange,[11, 54] and ultrafast thermal annealing (UTA)[27] seem to work effectively for many functional nanohybrids we have fabricated.

Light-assisted vacuum anneal could be operated at room temperature by placing the sample under illumination in vacuum typically ~ 10^{-6} Torr or better. A systematic shift of the Dirac point of graphene towards zero, which accelerates monotonically with increasing illumination time and intensity, has been observed during the annealing.[53] This confirms the removal of polar molecules adsorbed at the nanohybrid interface and their role as interface charge traps since a much enhanced photoresponse in both amplitude and speed was observed on the samples after the annealing. Ligand exchange has been extensively explored for replacing the ligands used in synthesis of QDs with ones that can provide better passivation of the QDs. In QDs/graphene nanohybrids, an additional consideration of the replacing ligand selection is their electrical conductivity for serving as the QD-QD (if a few QD layers are present) and QD/graphene charge transfer pathways. With adequate electric conduction, such ligands can lead to quench of the photoluminescence (PL), indicative of effective charge transfer out of QDs as required for QDs/graphene nanohybrids optoelectronics.[11] The UTA process exposes samples to high temperatures (up to 800 °C) for a short period of 1-3 seconds for refurbish the surface of the nanostructure sensitizers and their interfaces. For oxides nanohybrids, the UTA treatment in air was found to reduce the dark current and enhance photocurrent. In particular, graphene remains intact under the in-air UTA treatment.[27]

2.4 Sample characterization

Sample characterization was at two different levels. One is on the component level to analyze the morphology, dimension, crystallinity, chemical composition, optical and electronic properties. The other is on the device level after the heterostructures nanohybrids photodetectors were fabricated to analyze the device performance. In the former, scanning and transmission electron microscopy with energy dispersive x-ray spectroscopy (SEM, TEM, EDS), atomic force microscopy (AFM), confocal Raman spectroscopy, x-ray diffraction (XRD), optical spectroscopy in the spectral range of ultraviolet, visible to infrared, and Fourier-transform infrared spectroscopy (FTIR), etc. were used. In the latter, the electric transport properties, including I-V characteristic, noise, dynamic photoresponse, spectral responsivity, were characterized in a vacuum probe station using a semiconductor analyzer, spectrum analyzer when devices are illuminated with various lights sources and a monochromatic spectrometer system.

3. RESULT AND DISCUSSIONS

3.1 Critical role of interface in heterojunction nanohybrid optoelectronic properties

2D nanosheet/graphene is advantageous for heterostructures of different materials since it eliminates the stringent requirement of lattice match in heteroepitaxy. The emerging 2D materials, especially the TMDCs,[30] provide excellent opportunity of sensitizer design for IR detector. One focus of our research in 2D nanosheet/GFET is on an atomic-scale control of the vdW interface dipole-dipole coupling to ensure 1) a build-in electric field which is crucial to exciton dissociation to free carriers and carrier injection into GFET, which directly affects the EQE or gain and hence D* by orders of magnitude; 2) minimal charge trapping at the interface for fast photoresponse. We have explored several approaches in engineering the QD surface and QD/GFET vdW interface using both physical and chemical methods[9, 29, 55] and have demonstrated that both gain and response time can be improved by several orders of magnitude at a clean and engineered vdW interface. **Fig. 2a** depicts an example of III-V GaSe nanosheets (or 2D QDs)/GFET devices (left) with the interface build-in electric field anticipated from electronic structures of GaSe-QD and graphene (middle) that is in favor of the hole transfer from GaSe to graphene. However, the GaSe-QDs printed to the GFET channel often form an interface that may be contaminated by various chemicals, solvents and even air molecules used in the processing and printing of the GaSe-QDs, which can reduce the interface build-in electric field critical to exciton dissociation, block charge transfer across the interface and trap the charge to yield a slow response. This interface effect is clearly demonstrated in the improved dynamic photoresponse shown in **Fig. 2b (left)** after (black) the interface cleaning using a process we have developed as compared with that before (blue) the interface cleaning **Fig. 2b (right)**.[29] Moreover, the clean vdW GaSe/GFET interface has also yielded high gain (or EQE) in the range of 10^7-10^8 and visible detectivity D* up to $7x10^{13}$ Jones. It should be pointed out that this work demonstrates, for the first time, that high D* and fast photoresponse (symmetric 10-12 ms for rise and fall time constants) can be achieved simultaneously, suggesting the 2D nanosheet/GFET vdW heterostructure devices provide a promising scheme for photodetection.

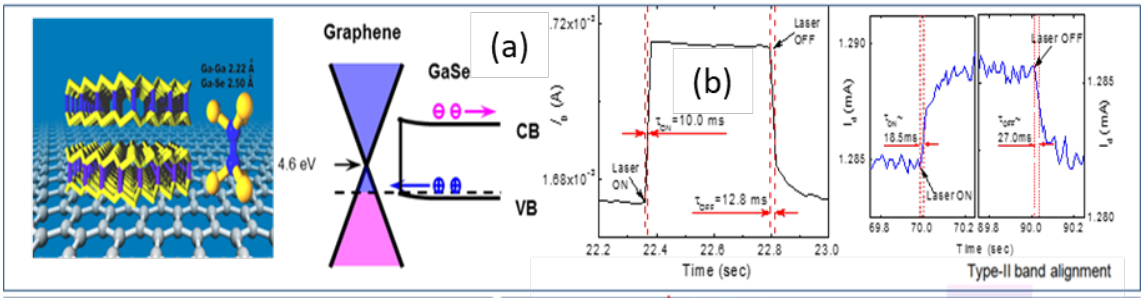

Figure 2 (a) Schematic of GaSe nanosheet/GFET device (left) with the build-in field across the GaSe/graphene vdW interface (middle) that affects the photoresponse amplitude and speed as shown from higher photoresponse and shorter response time of ~10-12 ms after interface cleaning (black) as compared to 18.5-27 ms before the cleaning (blue);

3.2 Plasmonic QDs/GFET SWIR detectors

The strong light wavelength selectivity determined by the LSPR frequency of the plasmonic QDs provides a viable wavelength tuning mechanism, allowing uncooled IR detection with reduced dark current.[31] The LSPR frequency may be tuned by n- or p-doping of semiconductors of reasonable bandgaps that are large enough to not contribute substantial dark current at room temperature.[31] In a recent work on $Fe_{1-x}S_2$ QDs (E_g~0.95 eV at x=0), we have demonstrated strong LSPR in NIR to SWIR spectra via doping of these QDs (**Fig. 3**). On the $Fe_{0.92}S_2$ QD/GFET devices, high responsivity up to $8x10^6$ A/W and D* near 10^{13} Jones have been demonstrated recently at SWIR (see **Fig. 3f**).[12] This is the first demonstration of the plasmonic QD/GFET photodetectors and the red-shifted spectral range and high detector performance suggests plasmonic-QD/GFET may provide a promising pathway to longer wavelengths beyond the SWIR spectrum in IR detection with much reduced dark current. A systematic study on the $Fe_{1-x}S_2$ QD/GFET devices has revealed that a shape control over these QDs can also red shift the plasmon resonance frequency to SWIR range for high

performance uncooled IR detection.[13] In addition, doped narrow-bandgap PbS and InSb QDs have also been investigated for IR detection.

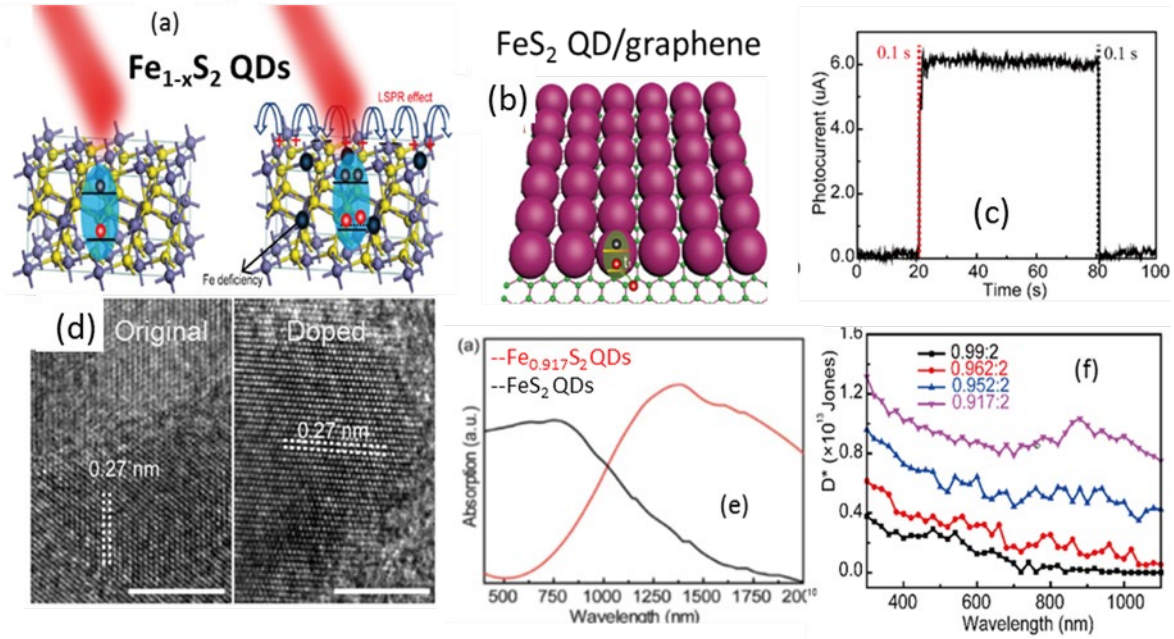

Figure 3 (a) Crystal structure of stoichiometric (left) FeS_2 exhibiting traditional semiconducting property under light irradiation and $Fe_{1-x}S_2$ with Fe deficiencies (right) and doped holes for LSPR effect under broadband light irradiation. Iron, sulfur atoms and iron deficiencies are depicted in blue, yellow and black, respectively. (b) schematic of $Fe_{1-x}S_2$ QD/GFET obtained using inkjet printing. (c) Dynamic response of a $Fe_{1-x}S_2$ QD/GFET at 1000 nm light. (d) HRTEM images and (e) absorption spectra of $Fe_{1-x}S_2$ QDs with Fe:S ratios of 0.99:2 (left) and 0.917:2 (right), respectively. (f) D* vs. wavelength measured on $Fe_{1-x}S_2$ QD/GFET nanohybrids with different x values.

3.3 2D atomic sheet stacks for NIR and SWIR detection

Figs. 4a-b illustrate two different IR detectors we have explored based on vdW stacks of 2D atomic sheets. **Fig. 4a** depicts a 2D p-$MoTe_2$ (E_g~1.0 eV)/graphene/n-SnS_2 (E_g~2.2 eV) p-g-n junction made by layer-by-layer stacking of different 2D atomic sheets together.[56] The insertion of the graphene between the p and n layers has been found critical to the interface quality for exciton dissociation and charge transport. At the optimal range of 5-7 graphene layers in this p-g-n devices, an extraordinary broadband responsivity exceeding 2.6×10^3 A/W and D^* up to ~10^{13} Jones in the UV-visible-NIR spectrum.[56] In addition, this device illustrates the viability in pairing 2D nanosheets of semiconductors of different, but complementary E_g and electronic structures to facilitate charge transport as shown in the inset of **Fig. 4a.** In a more recent study of the vdW heterostructure photodetectors for SWIR detection,[57] we have employed GaTe (E_g~1.0 eV) and γ-InSe (rhombohedral) with E_g in the range of 1.20 to 1.80 eV depending on the layer number of the InSe (**Fig. 4b)**. The ideal band diagram of the GaTe/InSe interface indicates that the GaTe/InSe vdW heterostructures is expected to type-II band alignment,[58-61] in which the interlayer transition energy of ~0.55 eV lies in the SWIR light range of 1.0−1.55 μm beyond the cut-off wavelengths of the individual GaTe and InSe. We have demonstrated that this GaTe/InSe vdW heterostructures photodetector shows an unprecedented D^* over a wide spectrum in ultraviolet (UV)-vis-NIR-SWIR light. Especially, the D^* of the photodetector can reach up to a record of 10^{14} Jones and 10^{12} Jones for 1064 nm and 1550 nm SWIR illumination at room temperature.

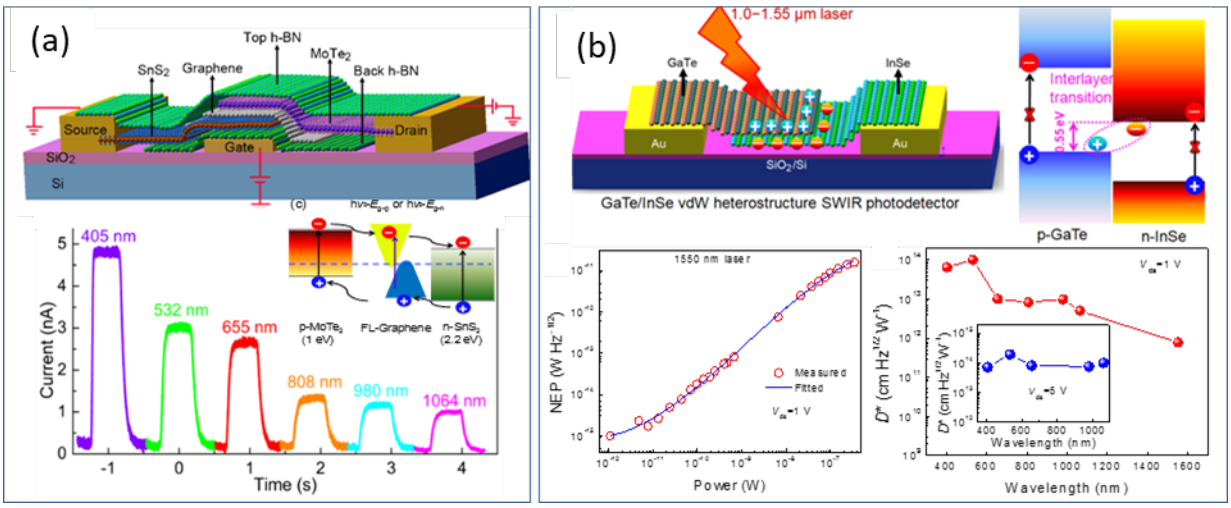

Figure 4 (a) Schematic h-BN/$MoTe_2$/graphene/SnS_2/h-BN device configuration and schematic band diagram and photoexcited carriers transport of the $MoTe_2$/graphene/SnS_2 vdW heterostructures. The $E_{g\text{-}p}$ and $E_{g\text{-}n}$ represent the band gap of p-$MoTe_2$ and n-SnS_2, respectively. Here, FL-graphene is a semi-metallic property which the Fermi level (at absolute zero) locates at above the bottom of the conduction band and below the top of the valence band due to the overlap of the conduction and valence bands. Dynamic response to light of different wavelengths in the range of 405 nm to 1064 nm are also included. (b) Schematic GaTe/InSe vdW heterostructure for SWIR photodetection. Left: 3D schematic of the GaTe/InSe photodetector configuration. Right: Schematic representation of the type-II band alignment of the GaTe/InSe vdW heterostructure and the corresponding principle of the interlayer transition at interface. The $E_{g\text{-}p}$ and $E_{g\text{-}n}$ are the bandgap of p-GaTe and n-InSe, respectively. (b) NEP calculated from the noise spectra as a function of illumination power under 1550 nm laser at V_{ds} = 1 V. (d) D^* as a function of the wavelength obtained at V_{ds} = 1 V and V_{ds} = 5 V (inset).

4. CONCLUSIONS

In summary, optoelectronic nanohybrids involving graphene and quantum nanostructures, such as quantum dots, nanotubes, nanosheets, have recently emerged as a unique scheme for high-performance photodetection. These nanohybrids have distinctive advantages over conventional semiconductors because of: 1) the strong quantum confinement in nanostructures which yields superior properties including high light absorption, spectra tunability, and reduced dark current due to suppressed phonon scattering; 2) exciton dissociation and charge transfer at the nanohybrid interface build-in field for efficient photo-carrier generation; and 3) high photoconductive gain and external quantum efficiency proportional to the ratio between the carrier lifetime enhanced by the quantum confinement in the nanostructures and the extremely short charge transit time due to the high mobility of graphene. These advantages make nanohybrids highly promising for designing uncooled quantum infrared detectors with high detectivity, high speed, low-cost and scalability. Besides high performance and low cost, the nanohybrid approach also has the advantage in its compatibility with Si-based readout circuits with micro/nanofabrication schemes employed for scaling up in practical applications.

Nevertheless, research on nanohybrids IR detectors has just begun and many important issues remain. First, controlling the surface of the sensitizer nanostructures and the interfaces involved in the heterostructures nanohybrids is critical to further improvement of the nanohybrid optoelectronic performance. Specifically, poor quality of these surfaces and interfaces would lead to formation of charge traps that can reduce the photoresponse and response speed, both are critical to commercial IR detectors and imaging systems. Development of new approaches to achieve an atomic control on these surfaces and interfaces represents an important task in future research on nanohybrids optoelectronics including IR detectors. Furthermore, development of suitable nanostructured sensitizers for longer wavelengths beyond SWIR spectrum is important in future research on uncooled MWIR to LWIR nanohybrid detectors. Finally, various light management schemes, such as plasmonic nanostructures and metamaterials that are effective in IR spectrum, may provide promising approaches to dramatically enhanced IR absorption and hence high response.

ACKNOWLEDGEMENTS

This research was supported in part by ARO Contract No. ARO-W911NF-16-1-0029 and NSF Contract Nos. NSF-ECCS-1809293, NSF-DMR-1909292, and NSF-DMR-1508494.

REFERENCE

1. J. Z. Wu, "Graphene", in *Transparent Conductive Materials. Materials, Synthesis and Characterization*, edited by D. L. a. D. E. Castellón (Wiley-VCH, 2019), Vol. Vol. 1 & 2, pp. 165-192.
2. K. S. Novoselov, A. K. Geim, S. V. Morozov, D. Jiang, Y. Zhang, S. V. Dubonos, I. V. Grigorieva and A. A. Firsov, "Electric field effect in atomically thin carbon films", *Science* **306** (5696), 666-669 (2004).
3. K. S. Novoselov, A. K. Geim, S. V. Morozov, D. Jiang, M. I. Katsnelson, I. V. Grigorieva, S. V. Dubonos and A. A. Firsov, "Two-dimensional gas of massless Dirac fermions in graphene", *Nature* **438** (7065), 197-200 (2005).
4. Y. B. Zhang, Y. W. Tan, H. L. Stormer and P. Kim, "Experimental observation of the quantum Hall effect and Berry's phase in graphene", *Nature* **438** (7065), 201-204 (2005).
5. P. Avouris, Z. H. Chen and V. Perebeinos, "Carbon-based electronics", *Nature Nanotechnology* **2** (10), 605-615 (2007).
6. C. R. Dean, A. F. Young, I. Meric, C. Lee, L. Wang, S. Sorgenfrei, K. Watanabe, T. Taniguchi, P. Kim, K. L. Shepard and J. Hone, "Boron nitride substrates for high-quality graphene electronics", *Nature Nanotechnology* **5** (10), 722-726 (2010).
7. J. H. Chen, C. Jang, S. D. Xiao, M. Ishigami and M. S. Fuhrer, "Intrinsic and extrinsic performance limits of graphene devices on SiO2", *Nature Nanotechnology* **3** (4), 206-209 (2008).
8. G. Konstantatos, M. Badioli, L. Gaudreau, J. Osmond, M. Bernechea, F. P. G. de Arquer, F. Gatti and F. H. L. Koppens, "Hybrid graphene-quantum dot phototransistors with ultrahigh gain", *Nature Nanotechnology* **7** (6), 363-368 (2012).
9. M. Gong, Liu, Qingfeng, Cook, Brent, Ewing, Daniel, Casper, Matthew, Stramel, Wu, Judy "All-printable ZnO quantum dots/Graphene van der Waals heterostructures for ultrasensitive detection of ultraviolet light", *ACS nano* **11** (4), 4114 (2017).
10. M. Gong, Q. Liu, R. Goul, D. Ewing, M. Casper, A. Stramel, A. Elliot and J. Z. Wu, "Printable Nanocomposite FeS2-PbS Nanocrystals / Graphene Heterojunction Photodetectors for Broadband Photodetection", *ACS Appl Mater Interfaces* **9**, 27801–27808 (2017).
11. M. G. Gong, R. Sakidja, R. Goul, D. Ewing, M. Casper, A. Stramel, A. Elliot and J. Z. Wu, "High-Performance All-Inorganic CsPbCl3 Perovskite Nanocrystal Photodetectors with Superior Stability", *Acs Nano* **13** (2), 1772-1783 (2019).
12. M. Gong, D. Ewing, M. Casper, A. Stramel, A. Elliot and J. Z. Wu, "Controllable Synthesis of Monodispersed Fe1- xS2 Nanocrystals for High-Performance Optoelectronic Devices", *ACS Appl Mater Interfaces* **11** (21), 19286-19293 (2019).
13. M. Gong, R. Sakidja, Q. Liu, R. Goul, D. Ewing, M. Casper, A. Stramel, A. Elliot and J. Z. Wu, "Broadband Photodetectors: Broadband Photodetectors Enabled by Localized Surface Plasmonic Resonance in Doped Iron Pyrite Nanocrystals (Advanced Optical Materials 8/2018)", *Advanced Optical Materials* **6** (8), 1870033 (2018).
14. B. Cook, Q. F. Liu, J. W. Liu, M. G. Gong, D. Ewing, M. Casper, A. Stramel and J. D. Wu, "Facile zinc oxide nanowire growth on graphene via a hydrothermal floating method: towards Debye length radius nanowires for ultraviolet photodetection", *Journal of Materials Chemistry C* **5** (38), 10087-10093 (2017).
15. J. Liu, R. Lu, G. Xu, J. Wu, P. Thapa and D. Moore, "Development of a Seedless Floating Growth Process in Solution for Synthesis of Crystalline ZnO Micro/Nanowire Arrays on Graphene: Towards High-Performance Nanohybrid Ultraviolet Photodetectors", *Advanced Functional Materials* **23** (39), 4941-4948 (2013).
16. F. Xia, H. Wang, D. Xiao, M. Dubey and A. Ramasubramaniam, "Two-dimensional material nanophotonics", *Nature Photonics* **8**, 899-907 (2014).
17. A. K. Geim and I. V. Grigorieva, "Van der Waals heterostructures", *Nature* **499** (7459), 419-425 (2013).
18. K. Roy, M. Padmanabhan, S. Goswami, T. P. Sai, G. Ramalingam, S. Raghavan and A. Ghosh, "Graphene–MoS2 hybrid structures for multifunctional photoresponsive memory devices", *Nature Nanotechnology* **8**, 826-830 (2013).

19. U. Bockelmann, "ELECTRONIC RELAXATION IN QUASI-ONE-DIMENSIONAL AND ZERO-DIMENSIONAL STRUCTURES", *Semiconductor Science and Technology* **9** (5), 865-870 (1994).
20. D. M. T. Kuo, A. B. Fang and Y. C. Chang, "Theoretical modeling of dark current and photo-response for quantum well and quantum dot infrared detectors", *Infrared Physics & Technology* **42** (3-5), 433-442 (2001).
21. V. J. Logeeswaran, J. Oh, A. P. Nayak, A. M. Katzenmeyer, K. H. Gilchrist, S. Grego, N. P. Kobayashi, S. Y. Wang, A. A. Talin, N. K. Dhar and M. S. Islam, "A Perspective on Nanowire Photodetectors: Current Status, Future Challenges, and Opportunities", *Ieee Journal of Selected Topics in Quantum Electronics* **17** (4), 1002-1032 (2011).
22. S. Keuleyan, E. Lhuillier, V. Brajuskovic and P. Guyot-Sionnest, "Mid-infrared HgTe colloidal quantum dot photodetectors", *Nature Photonics* **5** (8), 489-493 (2011).
23. S. Keuleyan, E. Lhuillier and P. Guyot-Sionnest, "Synthesis of Colloidal HgTe Quantum Dots for Narrow Mid-IR Emission and Detection", *Journal of the American Chemical Society* **133** (41), 16422-16424 (2011).
24. E. Lhuillier, S. Keuleyan, P. Rekemeyer and P. Guyot-Sionnest, "Thermal properties of mid-infrared colloidal quantum dot detectors", *Journal of Applied Physics* **110** (3) (2011).
25. H. Chen, X. Sun, K. W. C. Lai, M. Meyyappan and N. Xi,"Infrared Detection Using an InSb Nanowire", in *2009 IEEE Nanotechnology Materials and Devices Conference* (Traverse City, Michigan, USA, 2009), pp. 212.
26. M. I. Khan, X. Wang, X. Y. Jing, K. N. Bozhilov and C. S. Ozkan, "Study of a Single InSb Nanowire Fabricated via DC Electrodeposition in Porous Templates", *Journal of Nanoscience and Nanotechnology* **9** (4), 2639-2644 (2009).
27. Q. Liu, M. Gong, B. Cook, D. Ewing, M. Casper, A. Stramel and J. Wu, "Fused Nanojunctions of Electron-Depleted ZnO Nanoparticles for Extraordinary Performance in Ultraviolet Detection", *Advanced Materials Interfaces* (2017).
28. J. W. Liu, R. T. Lu, G. W. Xu, J. Wu, P. Thapa and D. Moore, "Development of a Seedless Floating Growth Process in Solution for Synthesis of Crystalline ZnO Micro/Nanowire Arrays on Graphene: Towards High-Performance Nanohybrid Ultraviolet Photodetectors", *Advanced Functional Materials* **23** (39), 4941-4948 (2013).
29. R. T. Lu, J. W. Liu, H. F. Luo, V. Chikan and J. Z. Wu, "Graphene/GaSe-Nanosheet Hybrid: Towards High Gain and Fast Photoresponse", *Scientific Reports* **6**, 19161 (2016).
30. Q. F. Liu, B. Cook, M. G. Gong, Y. P. Gong, D. Ewing, M. Casper, A. Stramel and J. D. Wu, "Printable Transfer-Free and Wafer-Size MoS2/Graphene van der Waals Heterostructures for High-Performance Photodetection", *Acs Appl Mater Inter* **9** (14), 12728-12733 (2017).
31. J. M. Luther, P. K. Jain, T. Ewers and A. P. Alivisatos, "Localized surface plasmon resonances arising from free carriers in doped quantum dots", *Nature Materials* **10** (5), 361-366 (2011).
32. M. Gong, R. Sakidja, Q. Liu, R. Goul, D. Ewing, M. Casper, A. Stramel, A. Elliot and J. Z. Wu, "Broadband Photodetectors Enabled by Localized Surface Plasmonic Resonance in Doped Iron Pyrite Nanocrystals", *Advanced Optical Materials*, 1701241 (2018).
33. B. Cook, Q. F. Liu, M. G. Gong, D. Ewing, M. Casper, A. Stramel and J. Wu, "Quantum Dots-Facilitated Printing of ZnO Nanostructure Photodetectors with Improved Performance", *Acs Appl Mater Inter* **9** (27), 23189-23194 (2017).
34. B. Cook., Gong, M.G., Ewing, D., Casper, M., Stramel, A., Elliot, A., Wu, J.Z., "Inkjet-Printing Multi-Color Pixilated Quantum Dots on Graphene for Broadband Photodetection", *ACS Applied Nano Materials* **2**, 3246 (2019).
35. J. Z. Wu, "Graphene", in *Transparent Conductive Materials. Materials, Synthesis and Characterization*, edited by D. L. a. D. E. Castellón (Wiley-VCH, 2018), Vol. Vol. 1 & 2.
36. E. L. Dereniak and G. D. Boreman, *Infrared Detectors and Systems*. (John Willey & Sons,, New York, USA, 1996).
37. J. Caniou, *Passive Infrared Detection-Theory and Applications* (Kluwer Academic, Boston, USA, 1999).
38. M. Henini and M. Razeghi, *Handbook of Infrared Detection Technologies*. (Elsevier Science, New York, 2002).
39. M. A. Kinch, *Fundamentals of Infrared Detector Materials* (SPIE Press,, Washington, USA, 2007).
40. A. Rogalski, *Infrared Detectors (Second Edition)*. (CRC Press, Boca Raton, FL, 2011).
41. Q. F. Liu, Y. P. Gong, J. S. Wilt, R. Sakidja and J. Wu, "Synchronous growth of AB-stacked bilayer graphene on Cu by simply controlling hydrogen pressure in CVD process", *Carbon* **93**, 199-206 (2015).
42. J. Liu, G. Xu, C. Rochford, R. Lu, J. Wu, C. M. Edwards, C. L. Berrie, Z. Chen and V. A. Maroni, "Doped graphene nanohole arrays for flexible transparent conductors", *Applied Physics Letters* **99** (2), 023111 (2011).
43. Q. Liu, Y. Gong, T. Wang, W.-L. Chan and J. Wu, "Metal-catalyst-free and controllable growth of high-quality monolayer and AB-stacked bilayer graphene on silicon dioxide", *Carbon* **96**, 203-211 (2016).

44. G. W. Xu, R. T. Lu, J. W. Liu, H. Y. Chiu, R. Q. Hui and J. Z. Wu, "Photodetection Based on Ionic Liquid Gated Plasmonic Ag Nanoparticle/Graphene Nanohybrid Field Effect Transistors", *Advanced Optical Materials* **2** (8), 729-736 (2014).
45. M. Alamri, R. Sakidja, R. Goul, S. Ghopry and J. Z. Wu, "Plasmonic Au Nanoparticles on 2D MoS2/Graphene van der Waals Heterostructures for High-Sensitivity Surface-Enhanced Raman Spectroscopy", *ACS Applied Nano Materials* **2** (3), 1412-1420 (2019).
46. M. Alamri, M. Gong, B. Cook, R. Goul and J. Z. Wu, "Plasmonic WS2 Nanodiscs/Graphene van der Waals Heterostructure Photodetectors", *Acs Appl Mater Inter* **11** (36), 33390-33398 (2019).
47. S. A. Ghopry, M. A. Alamri, R. Goul, R. Sakidja and J. Z. Wu, "Extraordinary Sensitivity of Surface-Enhanced Raman Spectroscopy of Molecules on MoS2 (WS2) Nanodomes/Graphene van der Waals Heterostructure Substrates", *Advanced Optical Materials* **7** (8), 1801249 (2019).
48. S. A. Ghopry, M. Alamri, R. Goul, B. Cook, S. M. Sadeghi, R. R. Gutha, R. Sakidja and J. Z. Wu, "Au Nanoparticle/WS2 Nanodome/Graphene van der Waals Heterostructure Substrates for Surface-Enhanced Raman Spectroscopy", *ACS Applied Nano Materials* **3** (3), 2354-2363 (2020).
49. M. Gong, A. Kirkeminde, Y. Xie, R. Lu, J. Liu, J. Wu and S. Q. Ren, "Iron Pyrite (FeS2) Broad Spectral and Magnetically Responsive Photodetectors", *Advanced Optical Materials* **1**, 78-83 (2013).
50. B. Liu, R. R. Gutha, B. Kattel, M. Alamri, M. Gong, S. M. Sadeghi, W.-L. Chan and J. Z. Wu, "Using Silver Nanoparticles-Embedded Silica Metafilms as Substrates to Enhance the Performance of Perovskite Photodetectors", *Acs Appl Mater Inter* **11** (35), 32301-32309 (2019).
51. M. Gong, A. Kirkeminde, N. Kumar, H. Zhao and S. Ren, "Ionic-passivated FeS2 photocapacitors for energy conversion and storage", *Chem. Commun.* **49** (81), 9260-9262 (2013).
52. M. Gong, A. Kirkeminde and S. Ren, "Symmetry-defying iron pyrite (FeS_2) nanocrystals through oriented attachment", *Sci Rep* **3**, 2092 (2013).
53. Y. Zhang, G. Hu, M. Gong, M. Alamri, C. Ma, M. Liu and J. Z. Wu, "Lateral Graphene p–n Junctions Realized by Nanoscale Bipolar Doping Using Surface Electric Dipoles and Self-Organized Molecular Anions", *Advanced Materials Interfaces* **6** (1), 1801380 (2019).
54. M. G. Gong, Q. F. Liu, R. Goul, D. Ewing, M. Casper, A. Stramel, A. Elliot and J. Z. Wu, "Printable Nanocomposite FeS2-PbS Nanocrystals/Graphene Heterojunction Photodetectors for Broadband Photodetection", *Acs Appl Mater Inter* **9** (33), 27801-27808 (2017).
55. M. Gong, R. Sakidja, R. Goul, D. Ewing, M. Casper, A. Stramel, A. Elliot and J. Z. Wu, "High-Performance All-Inorganic CsPbCl3 Perovskite Nanocrystal Photodetectors with Superior Stability", *ACS Nano* **13** (2), 1772-1783 (2019).
56. A. Li, Q. Chen, P. Wang, Y. Gan, T. Qi, P. Wang, F. Tang, J. Z. Wu, R. Chen, L. Zhang and Y. Gong, "Ultrahigh-Sensitive Broadband Photodetectors Based on Dielectric Shielded MoTe2/Graphene/SnS2 p–g–n Junctions", *Advanced Materials* **31** (6), 1805656 (2019).
57. T. Qi, Y. Gong, A. Li, X. Ma, P. Wang, R. Huang, C. Liu, R. Sakidja, J. Z. Wu, R. Chen and L. Zhang, "Interlayer Transition in a vdW Heterostructure toward Ultrahigh Detectivity Shortwave Infrared Photodetectors", *Advanced Functional Materials* **30** (3), 1905687 (2020).
58. W. Feng, Z. Jin, J. Yuan, J. Zhang, S. Jia, L. Dong, J. Yoon, L. Zhou, R. Vajtai, J. M. Tour, P. M. Ajayan, P. Hu and J. Lou, "A fast and Zero-Biased Photodetector Based on GaTe-InSe Vertical 2D p-n Heterojunction", *2d Mater* **5** (2), 025008 (2018).
59. P. Matheswaran, R. Sathyamoorthy and K. Asokan, "Schottky Nature of InSe/Cu Thin Film Diode Prepared by Sequential Thermal Evaporation", *Electron Mater Lett* **8** (6), 621−626 (2012).
60. F. Wang, Z. X. Wang, K. Xu, F. M. Wang, Q. S. Wang, Y. Huang, L. Yin and J. He, "Tunable GaTe-MoS2 van der Waals p-n Junctions with Novel Optoelectronic Performance", *Nano Letters* **15** (11), 7558-7566 (2015).
61. V. N. Katerinchuk and M. Z. Kovalyuk, "Gallium Telluride Heterojunctions", *Tech Phys Lett+* **25** (1), 54−55 (1999).